Point defect engineering strategies to suppress A-center formation in silicon

A. Chroneos,[1] C. A. Londos,[2,a)] E. N. Sgourou,[2] and P. Pochet[3,b)]
[1]*Department of Materials, Imperial College London, London SW7 2AZ, United Kingdom*
[2]*Solid State Physics Section, University of Athens, Panepistimiopolis Zografos, Athens 157 84, Greece*
[3]*Laboratoire de Simulation Atomistique (L_Sim), SP2M, INAC, CEA-UJF, 38054 Grenoble Cedex 9, France*

(Received 27 September 2011; accepted 11 November 2011; published online 12 December 2011)

We investigate the impact of tin doping on the formation of vacancy-oxygen pairs (*V*O or A-centers) and their conversion to VO_2 clusters in electron-irradiated silicon. The experimental results are consistent with previous reports that Sn doping suppresses the formation of the A-center. We introduce a model to account for the observed differences under both Sn-poor and Sn-rich doping conditions. Using density functional theory calculations, we propose point defect engineering strategies to reduce the concentration of the deleterious A-centers in silicon. We predict that doping with lead, zirconium, or hafnium will lead to the suppression of the A-centers. © *2011 American Institute of Physics*. [doi:10.1063/1.3666226]

Silicon (Si) is widely used in a range of applications; however, the detailed understanding of numerous defect-dopant interactions affecting its properties is not well established.[1] These become increasingly important as the dimensions of devices are a few nanometers with atomic effects coming into play.

Oxygen (O) is one of the most significant impurities in Czochralski-Si (Cz-Si) and is introduced during crystal growth. Oxygen intersitials (O_i) readily trap lattice vacancies (*V*) forming *V*O pairs. Thereafter, these A-centers anneal at about 300 °C to form larger clusters (VO_2).[2] A-centers are both electrically and optically active (whereas VO_2 clusters are only optically active) and it is technologically important to suppress their formation.[3,4] Previous experimental studies determined that isovalent impurities such as tin (Sn) can modify the formation processes of A-centers in Si.[4] Sn is introduced in Si or Ge at ever increasing concentrations to modify their lattice parameter and electronic properties.[5] Here, we investigate the impact of Sn doping on the formation of *V*O and its conversion to VO_2 defect in electron-irradiated Cz-Si. We introduce point defect engineering strategies to suppress the concentration of *V*O and related clusters in Si.

Figure 1 demonstrates the evolution with temperature of the *V*O and VO_2 bands for the Sn-poor and Sn-rich samples, respectively (details on the experimental methodology and the results are given in Ref. 6). The production of the A-center is suppressed in the Sn-rich sample consistently with previous experimental reports (Fig. 1).[7] The *V* formed during irradiation that did not recombine with self-interstitials can be captured by Sn impurities to form Sn*V* pairs. Sn effectively competes with O_i in capturing *V* and results in the reduction of the *V*O concentration. The Sn*V* pair dissociates via the reaction $SnV \rightarrow Sn + V$ at 170 °C. As it is IR inactive, its presence in the material can be noted by the increase of the concentration of the *V*O and the V_2 centers.[7] This is evident by the steep increase in the concentration of the absorption coefficient of *V*O at about 170 °C (Fig. 1). This is not observed in the Sn-poor case and indicates that for a low Sn-concentration the impact of Sn doping on the A-center is negligible. Importantly, we observe a decrease in the *V*O concentration of almost 30% at 250 °C, between the Sn-poor and Sn-rich samples (Fig. 1). As the initial oxygen concentration is the same in both samples, we can infer ~30% reduction for the surviving *V* after irradiation in the Sn-rich sample. This can be related to the ability of oversized impurities to act as recombination centers for intrinsic defects allowing the suppression of unwanted radiation-enhanced phenomena.[8] The differences in the C-concentrations between the samples (Fig. 1) may also

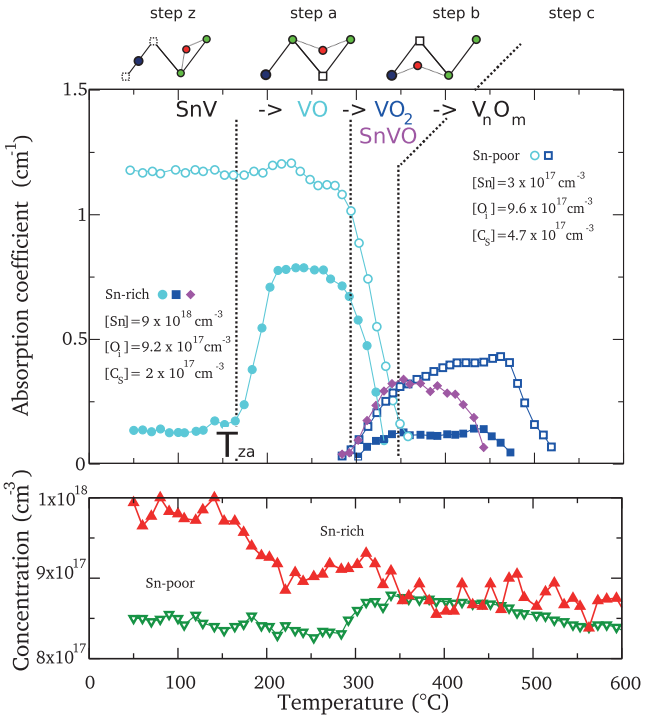

FIG. 1. (Color online) The thermal evolution of *V*O (cyan circles), VO_2 (dark blue squares), and SnVO (magenta diamonds) defects for Sn-poor (open symbols) and Sn-rich samples (solid symbols) are shown with the schematic of the 4-step model proposed. In the upper part, the underling defects are sketched using blue and green circles for the D impurity and Si atoms, square and dotted squares for the *V* and semi-*V*, and red circles for the oxygen atom. The bottom part of the figure represents the thermal evolution of the O_i for Sn-poor (open triangle) and Sn-rich (solid triangle) conditions.

a)Electronic mail: hlontos@phys.uoa.gr.
b)Author to whom correspondence should be addressed. Electronic mail: pascal.pochet@cea.fr.

affect the formation of *V*O.[9] The Sn-poor sample has more than double C-concentration as compared to the Sn-rich sample and this would lead to an increase of the *V*O concentration (reducing the ~30% difference).

Another important result is that the conversion of the *V*O to the VO_2 defect is reduced in the Sn-rich sample in comparison with the Sn-poor sample. The conversion ratio is reduced from 17% for the Sn-poor sample to 7.5% for the Sn-rich sample. This is due to the trapping of migrating *V*O pairs by Sn to form Sn*V*O clusters.[10]

For the Sn-poor sample, we propose a 3-step process scheme:

Step (a) up to 280 °C. Here, both *V*O and O_i concentrations are almost constant and VO_2 is not detected. All non-annihilated *V*, besides those pairing to form V_2 defects, are trapped by oxygen atoms. The *V*O and O_i concentrations are found to be $7.3 \times 10^{16}\,cm^{-3}$ and $8.4 \times 10^{17}\,cm^{-3}$, respectively.

Step (b) 350 °C > T > 280 °C. Both VO_2 and O_i quasi-linearly increase while *V*O decreases also quasi-linearly. We consider 4 elementary reactions

$$\text{(i) } VO + VO \rightarrow VO_2 + V;\ \text{(ii) } VO + Si_I \rightarrow O_i;$$
$$\text{(iii) } V + O_i \rightarrow VO;\ \text{(iv) } VO + O_i \rightarrow VO_2$$

The concomitant increase of VO_2 and O_i seems to exclude reaction (iii) or (iv) acting alone, while combining all four could compensate the formation of *V* to form further *V*O centers without decreasing the O_i concentration. Multiplying reaction (ii) by y and reaction (iv) by 4: $(4+y)\ VO + y\ Si_I \rightarrow 4\ VO_2 + (y-4)\ O_i$.

This reaction reproduces the observed concentration evolution in this temperature range for y values in-between 20 and 36. Indeed at 325 °C using Fig. 1, we calculated $\Delta[O_i] = 2 \times 10^{16}\,cm^{-3}$; $\Delta[VO_2] = 5 \times 10^{15}\,cm^{-3}$ $\Delta[VO] = 5 \times 10^{16}\,cm^{-3}$ leading to: $(y-4)/4 = 4$ for the $[O_i]/[VO_2]$ ratio $(y+4)/4 = 10$ for the $[VO]/[VO_2]$ ratio. From the first relation $y = 20$ and from the second $y = 36$. The results explain the unbalanced reaction between *V*O and VO_2 due to the predominance of reaction (ii) with respect to reaction (i) or reaction (iv), as revealed by the high value of y.[11] That is, the reaction of *V*O with Si_I is the dominant one. Sources of the Si_Is are large clusters of these defects formed during irradiation.[2]

Step (c) for T > 350 °C. Here, O_i starts to decrease while *V*O is no more detected and the VO_2 increase is reduced with respect to step (c). This is connected to the formation of larger V_nO_m ($n \geq 1$; $m > 2$) clusters through the reaction $VO_2 + (n-1)\ V + (m-2)\ O_i \rightarrow V_nO_m$ reducing the concentration of VO_2.

For the Sn-rich sample, we propose a 4-step process scheme (Fig. 1):

Step (z) for T < 150 °C. Here, both *V*O and O_i concentrations are almost constant. The *V*O concentration is reduced by almost one order of magnitude with respect to the Sn poor sample as most *V* are trapped by Sn atoms. The *V*O and O_i concentrations are calculated to be $8 \times 10^{15}\,cm^{-3}$ and $9.7 \times 10^{17}\,cm^{-3}$, respectively. In Fig. 1, the threshold temperature, T_{za}, between steps (z) and (a) is important (see below).

Step (a) 225 °C > T > 150 °C. Here, *V*O increases quasi-linearly while O_i decreases quasi-linearly. The latter evolution is due to the dissociation of Sn*V* followed by a re-association with O_i as indicated by the near opposite concentration evolution rate, $-1.2 \times 10^{17}\,cm^{-3}$/K and $4 \times 10^{16}\,cm^{-3}$/K for O_i and *V*O, respectively. At the end of the second step and up to about 275 °C, both *V*O and O_i concentrations reach constant values ($5 \times 10^{16}\,cm^{-3}$ and $9.1 \times 10^{17}\,cm^{-3}$, respectively). The reduction of about 30% of the *V*O concentration with respect to the Sn-poor sample is attributed to the equivalent reduction of the *V* in the mechanism proposed previously.[8]

Step (b) 325 °C > T > 280 °C. Both Sn*V*O and VO_2 quasi-linearly increase while *V*O decreases also quasi-linearly and O_i remains constant. 4 elementary reactions are considered

$$\text{(i) } VO + VO \rightarrow VO_2 + V;\ \text{(ii) } VO + Si_I \rightarrow O_i;$$
$$\text{(iii) } V + O_i \rightarrow VO;\ \text{(iv) } VO + Sn \rightarrow SnVO.$$

The main difference with regard to the Sn poor sample is the trapping of *V*O by Sn and the consecutive reduction of VO_2 formation. Thus, reaction $VO + O_i \rightarrow VO_2$ can be neglected here. Notably, a similar reduction of 30% of Si_I [and of reaction (ii)] should result from the above considerations on defect formation. For the evolution of the concentration rate in this temperature range, we multiply reactions (i) and (ii) by x and reaction (iv) by z: $(2x+z)\ VO + zSn + xSi_I \rightarrow zSnVO + xVO_2$.

This relation illustrates the complexity of reactions (i), (ii), and (iv) above. In particular, it illustrates the unbalanced conversion rates of *V*O defect to form the VO_2 center and the *V*O defect to form the Sn*V*O center.

Step (c) 400 °C > T > 325 °C. O_i decreases, *V*O is no more detected, and both are reduced with respect to step (b). This is linked to the formation of larger V_nO_m ($n \geq 1$; $m > 2$) clusters (through the reaction $VO_2 + (n-1)\ V + (m-2)\ O_i \rightarrow V_nO_m$) that reduces the concentration of VO_2. At the end of this step and for T > 400 °C, the O_i concentration reaches a plateau value, while both Sn*V*O and VO_2 signals vanish.

To model the system, we used density functional theory (DFT), the BigDFT code,[12] a supercell of 216 atoms and the parameters of previous studies.[13] We calculated the binding energies, E_b (defined by $E_b = E_{defect\ cluster} - \Sigma E_{isolated\ defects}$ under thermal equilibrium conditions), of the clusters of interest. Negative E_b imply that a cluster is energetically favorable with respect to its constituent isolated components. The energy barriers are calculated using the Nudged Elastic Band method as implemented in BigDFT.[12]

The E_b were calculated to be −1.17 eV and −1.53 eV for Sn*V* and *V*O, respectively (Table I). Thus, *V*O is more stable compared to Sn*V* at equilibrium conditions. To rationalize the experimental observations, we also calculate the first step of dissociation of the two centers. For *V*O center, configuration VO_{1NN} corresponds to a bond-centered oxygen first neighbour to the *V* as depicted by Furuhashi and Taniguchi.[14] We found an energy 0.48 eV higher than the A-center with a barrier energy of 0.90 eV (Table I) in line with the previous results.[14]

For Sn*V*, the situation is more complicated as it is stabilized in its split-*V* form, sSn*V*, the Sn atom being at the center of the split-*V*. The position with a *V* first neighbour of a Sn atom $Sn_{1NN}V$ is not stable and always relaxes toward the sSn*V*

TABLE I. Details of the DFT results for all four D impurities and oxygen. The energies are given in eV with respect to reference structures, sDV and VO, respectively. The calculated covalent radii of the substitutional impurities (last column) are given in pm. The corresponding defects configurations are sketched in Ref. 6.

sDV	$sD_{2NN}V$	$D_{2NN}V$	$D_{3NN}V$	$D_{\infty NN}V$	D_{sub}
Sn	0.82	0.68	1.12	1.17	127
Pb	0.83	0.76	1.30	1.37	129
Zr	—	—	2.55	2.89	130
Hf	—	—	2.86	4.38	130
VO	sVO_{1NN}	VO_{1NN}	VO_{2NN}	$VO_{\infty NN}$	Si
O	0.90	0.48	1.53	1.53	118

configuration. The first dissociation step corresponds to a configuration $Sn_{2NN}V$, where V is a second neighbour to the Sn atom (see Ref. 6). The calculated energy is 0.68 eV and therefore higher than the SnV center. The split-V configuration is 0.82 eV, that is only 0.14 eV higher that the $Sn_{2NN}V$ configuration (see Ref. 6). These results are consistent with the experimental observations as a first neighbour V to a Sn ($Sn_{2NN}V$ conf.) would need only energy of 0.14 eV to form the sSnV center. Conversely, energy of 0.42 eV is needed to form the VO for a V first neighbour of an O_i (VO_{1NN} conf.), leading to a kinetic stabilization of the SnV center with respect to the VO center. That is, the formation of the more stable VO center is prevented for low temperatures by the smaller activation needed to trap V in SnV centers. At high temperatures, V should be trapped by the more bounded VO centers.

The dissociation of SnV (170 °C) at lower temperatures compared to VO (280 °C) is consistent to the dissociation barrier (0.82 eV and 0.90 eV, respectively, Table I). Notably, an impurity D that would form a more bonded center with the V would result in the increase of the temperature range of step (z) where the VO concentration is an order of magnitude lower than in Sn poor sample.

The first attempt is with lead (Pb). The PbV center is also stabilized in its split-V form with an E_b of −1.37 eV, hence it is more stable than the SnV center but less stable than the VO center. For the first dissociation step, we found for $Pb_{2NN}V$ an energy 0.76 eV higher than the PbV center and for the corresponding barrier a value of 0.83 eV that is only 0.07 eV higher that the $Pb_{2NN}V$ configuration (Table I). The latter value is half than the one obtained for Sn and thus results in a stronger sink effect for V. Moreover, the slightly higher value of the barrier of the first dissociation step should also result in shift of the temperature threshold for step (a) in-between 200 and 300 °C, increasing the temperature range with low VO concentration (below T_{za}, Fig. 1). We attribute the reinforcement of this effect going from Sn to Pb to the increase of the covalent radius of the latter (Table I). This can be more significant by using dopants with larger radii such as hafnium (Hf) or zirconium (Zr).

The split-V configuration sDV is further favored with respect to the $D_{1NN}V$ configuration: 0.79 and 0.72 eV for Zr and Hf, respectively. Interestingly, the configuration $D_{2NN}V$, where the V is a second neighbour of the dopant atom, is no more stable with respect to the sDV configuration: starting from the $D_{2NN}V$ configuration, the system relaxes through the sDV configuration as in the case of the $D_{1NN}V$ configuration. This means that a V at a second neighbour to the D atom can form the D-split-V center without any activation. The V close to a D atom is only stable as a third neighbour with energies as high as 2.55 eV and 2.86 eV for Zr and Hf, respectively. This increase is in the line of bigger covalent radius (Table I). The high energies will result in stabilization of the sDV center preventing the formation of VO center up to $T_{za} = 350$ °C.

The inclusion of oversized dopants has been extensively investigated for metallic alloys under irradiation.[8] Interestingly, Zr and Hf proposed here are known to suppress the transient enhanced chromium diffusion.[8] In particular, they act as traps for point defects increasing the recombination rate and decreasing the number of surviving Frenkel pairs.[8]

The increase of T_{za} is the key for the proposed suppression strategy of the A-centers as it corresponds to a wider temperature range of step (z). Interestingly, if T_{za} reaches 350 °C, the release of Si_I (proposed to explain the observed unbalanced reaction between VO and VO_2) will favour a further reduction of the surviving Frenkel pairs. We propose to achieve this increase of T_{za} using oversized dopant such as Sn, Pb, Zr, or Hf.

The VO defect is largely suppressed in Sn-rich doped Si due to the capture of V by Sn atoms. This leads to the reduction of the conversion of VO to VO_2 due to the formation of SnVO clusters, which attract V with E_b higher than that of the A-center. Based on DFT calculations, we propose that doping Si with oversized dopants (Pb, Zr, or Hf) is the way to suppress the VO formation.

This work was partially funded by the French National Research Agency through the BOLID Project ANR-10-HABISOL-001. Calculation time was provided by the French GENCI Agency under Project No. t2011096107.

[1]D. Caliste and P. Pochet, Phys. Rev. Lett. **97**, 135901 (2006); D. Caliste, P. Pochet, T. Deutsch, and F. Lançon, Phys. Rev. B **75**, 125203 (2007); S. Takeuchi, Y. Shimura, O. Nakatsuka, S. Zaima, M. Ogawa, and A. Sakai, Appl. Phys. Lett. **92**, 231916 (2008); D. Caliste, K. Z. Rushchanskii, and P. Pochet, Appl. Phys. Lett. **98**, 031908 (2011).
[2]R. C. Newman and R. Jones, in *Oxygen in Silicon*, edited by F. Shimura, Semiconductors and Semimetals, (Academic, Orlando, 1994), Vol. 42, p. 289.
[3]J. W. Corbett, G. D. Watkins, and R. S. McDonald, Phys. Rev. **135**, A1381 (1964); C. A. Londos, Phys. Status Solidi A **92**, 609 (1985).
[4]G. D. Watkins, IEEE Trans. Nucl. Sci. **16**, 13 (1969); C. Claeys, E. Simoen, V. B. Neimash, A. Kraitchinskii, M. Kras'ko, O. Puzenko, A. Blondeel, and P. Clauws, J. Electrochem. Soc. **146**, G738 (2001).
[5]A. Chroneos, C. Jiang, R. W. Grimes, U. Schwingenschlögl, and H. Bracht, Appl. Phys. Lett. **94**, 252104 (2009); H. Tahini, A. Chroneos, R. W. Grimes, and U. Schwingenschlögl, Appl. Phys. Lett. **99**, 162103 (2011).
[6]See supplementary material at http://dx.doi.org/10.1063/1.3666226 for details regarding the experimental methodology, IR spectra, the thermal evolution of the defects, and sketch of the calculated configurations in Table I.
[7]B. G. Svensson, J. Svensson, G. Davies, and J. W. Corbett, Appl. Phys. Lett. **51**, 2257 (1987).
[8]N. Sakaguchi, S. Watanabe, and H. Takahashi, Nucl. Instrum. Methods Phys. Res. B **153**, 142 (1999).
[9]V. D. Ahmetov and V. V. Bolotov, Radiat. Eff. **52**, 149 (1980).
[10]L. I. Khirunenko, O. O. Koibzar, Yu. V. Pomozov, M. G. Sosnin, and M. O. Tripachko, Physica B **340–342**, 541 (2003).
[11]J. L. Lindström and B. G. Svensson, Mater. Res. Soc Symp. Proc. **59**, 45 (1986).
[12]L. Genovese, M. Ospici, T. Deutsch, J. F. Méhaut, A. Neelov, and S. Goedecker, J. Chem. Phys. **131**, 034103 (2009).
[13]E. Machado-Charry, L. K. Beland, D. Caliste, L. Genovese, T. Deutsch, N. Mousseau, and P. Pochet, J. Chem. Phys. **135**, 034102 (2011).
[14]M. Furuhashi and K. Taniguchi, Appl. Phys. Lett. **86**, 142107 (2005).